Proceedings of the
Annual Stability Conference
Structural Stability Research Council
San Antonio, Texas, March 19-22, 2024

On lateral-torsional buckling of steel I-section beams subjected to biaxial bending

David Henriques[1], Rodrigo Gonçalves[2]

Abstract
This paper investigates the lateral-torsional buckling behavior and strength of compact steel I-section beams subjected to biaxial bending (without axial force) and assess the accuracy of the Eurocode 3 beam-column interaction formulae for the buckling limit state. Particular focus is placed on the comparison between various support conditions (pinned, clamped, free) along the two principal planes. The load cases considered include point loads and end moments. This investigation relies on non-linear numerical results obtained using a geometrically exact beam element developed by one of the authors, which allows including the effects of geometric imperfections, plasticity, residual stresses, large displacements and finite rotations (including Wagner effects). The results obtained show that lateral-torsional buckling under biaxial moment can exhibit quite unexpected results — for instance, for the same slenderness and bending moment diagrams, preventing the lateral rotation at the support can lead to a lower strength — and that the Eurocode 3 interaction formulae can lead to unsafe results even in simple cases.

1. Introduction

The buckling behavior of columns, beams and beam-columns has been extensively investigated by many researchers, see e.g. the references listed in (Ziemian 2010). Most of the research concerns isolated and simply supported members — single span members with end "fork" conditions (null translations and torsional rotation, but free to warp) — albeit subjected to many different load cases. This is the case of the numerical studies that led to the proposal of the current beam-column interaction formulae in Eurocode 3 (CEN 2005; Boissonnade et al. 2006). The application of these formulae to other support cases was first investigated by the author (Gonçalves & Camotim 2004), for the in-plane case with axial compression and uniaxial bending, demonstrating that unsafe or excessively safe strength predictions can be obtained if the equivalent moment factor (C_m) is not judiciously selected, as the coded expressions essentially apply to the simply supported case.

This paper addresses the case of lateral-torsional buckling under biaxial bending (without axial force). Particular focus is placed on the effect of the boundary conditions (namely other than

[1] Structural Engineer, CERIS and PPE Structural Engineering, Portugal < dos.santos.henriques.david@gmail.com>
[2] Full Professor, CERIS and Universidade Nova de Lisboa, Portugal <rodrigo.goncalves@fct.unl.pt>

simply supported) and the cases shown in Fig. 1 are considered (*w* refers to the warping DOF). The two cross-sections selected are similar to those in other related research initiatives (e.g. Ofner 1997, Boissonnade et al. 2006), are not susceptible to local buckling (compact sections) and cover appropriate height/width ratios and residual stress patterns. Using the notation displayed in the bottom part of the figure, a beam support scheme is indicated in the format AB_yCD_z, where *A*,*C* are used for the left support and *B*,*D* for the right support, whereas the indices pertain to the bending plane (*y* vertical; *z* horizontal). For instance, SC_yCS_z, means that the left support is type S_y+C_z and the right support is type C_y+S_z.

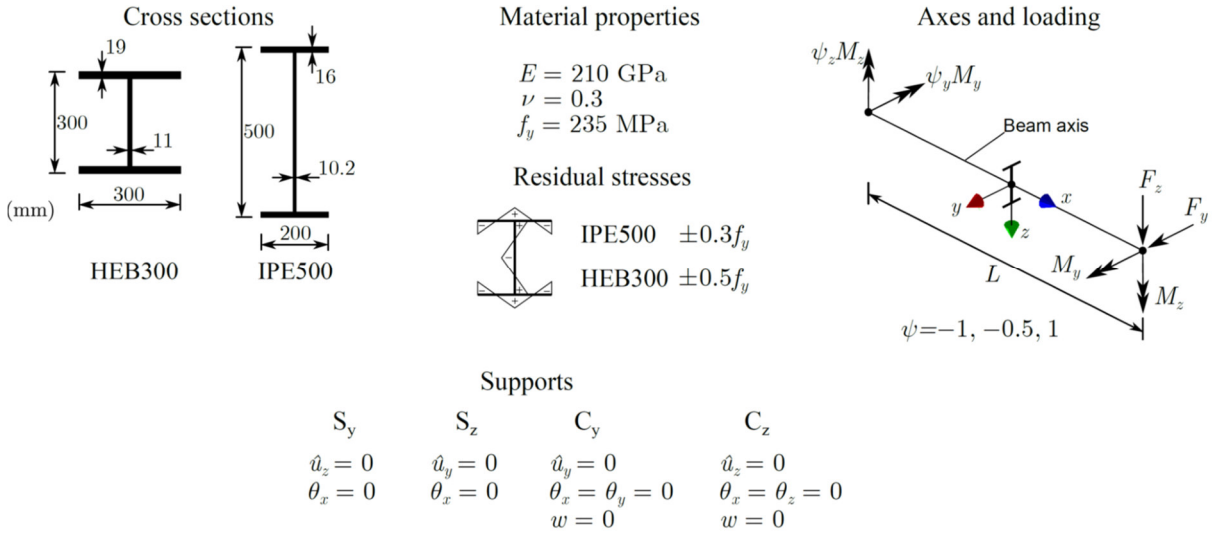

Figure 1: Cross-sections, material properties, residual stresses, loading and boundary conditions

The results of three analysis types are reported in the paper: GNA (Geometrically Non-linear Analyses), GMNA (Geometrically and Materially Non-linear Analyses) and GMNIA (Geometrically and Materially Non-linear Analyses with geometric imperfections and residual stresses). In the material non-linear cases, an elastic-perfectly plastic law is assumed. For the GMNIA analyses, a lateral single half-wave imperfection of amplitude $e_0 = L/1000$ is adopted, except in the cases with $\psi = -1$, in which case two half-waves are considered. The two directions for the imperfections are always investigated and only the lowest strength obtained is reported. It should be noted that the $\psi = -0.5$ case is of particular interest in this study, since it can be obtained with both SS and SC boundary conditions in that plane of bending, and therefore allows investigating the effect of varying the boundary conditions while maintaining the bending moment diagram shape.

The α parameter is introduced,

$$\alpha = \arctan\left(\frac{m_y}{m_z}\right), \tag{1}$$

where $m_i = M_i/M_{pl,i}$ is the non-dimensional moment acting about axis i and $M_{pl,i}$ is the corresponding full plastic moment. The GMNIA analyses carried out concern $\alpha = 0$ (minor axis bending), 11º, 22.5º, 45º, 67.5º, 79º and 90º (major axis bending).

The numerical results are obtained using the displacement-based geometrically exact beam finite element described, validated and applied in (Gonçalves 2019, 2020, 2022), which can handle large displacements and finite rotations, plasticity, residual stresses and Wagner effects. As proposed in these papers, the beams are modelled using 30 equal length finite elements and the cross-section integration is carried out with 11×3 (mid-line × thickness directions) Gauss points in each wall. The flange-web radius is neglected.

2. Buckling under M_y

First, the uniaxial (major axis, $\alpha = 90^o$) bending case is examined, since results for support conditions other than simply supported are not available in the literature (to the authors' best knowledge). Fig. 2 shows the lateral-torsional buckling reduction factors

$$\chi_{LT} = \frac{M_y^{GMNIA}}{M_{pl,y}}, \tag{2}$$

obtained for several loading and support conditions, grouped according to the corresponding ψ_y ratio, as well as the values (in the form of curves) obtained using the formulation which will be adopted in new version of Eurocode 3 for simply supported members (Taras & Greiner 2010, Greiner & Taras, 2010), reading

$$\begin{aligned} \chi_{LT} &= \frac{\varphi}{\Phi_{LT}+\sqrt{\Phi_{LT}^2-\varphi\bar{\lambda}_{LT}^2}} \leq 1, \\ \Phi_{LT} &= \frac{1}{2}\left[1+\varphi\left(\frac{\alpha_{LT}\bar{\lambda}_{LT}^2}{\bar{\lambda}_z^2}\left(\bar{\lambda}_z-0.2\right)+\bar{\lambda}_{LT}^2\right)\right], \end{aligned} \tag{3}$$

where the imperfection factor α_{LT} equals 0.34 for IPE500 and 0.27 for HEB300, $\varphi = 1.25 - 0.1\psi_y - 0.15\psi_y^2$ for linear bending moment diagrams between lateral supports, $\bar{\lambda}_{LT}$ is the non-dimensional slenderness for lateral-torsional buckling,

$$\bar{\lambda}_{LT} = \sqrt{\frac{M_{pl,y}}{M_{cr}}}, \tag{4}$$

with the critical bifurcation moment M_{cr} calculated from a linear stability analysis, and $\bar{\lambda}_z$ is the non-dimensional slenderness for weak-axis flexural buckling (as a column), calculated using for the buckling length the laterally unsupported length of the compression flange.

The small scatter in each graph evidences that, at least for the cases considered, the boundary conditions do not affect significantly the $\chi_{LT} - \bar{\lambda}_{LT}$ trend. For this reason, the new Eurocode 3 approach, even though it was developed for simply supported members with critical buckling mode shape imperfections, is found to provide quite accurate and generally safe χ_{LT} values if $\bar{\lambda}_z$ is calculated for a simply supported member with the same $\bar{\lambda}_{LT}$ value. Although there is a small scatter for $\psi_y = -0.5$, it should be noted that the CS_ySS_z case leads to slightly higher resistances, followed by the CS_yCS_z case, whereas the values for SS_yCS_z and SS_ySS_z virtually overlap (this is more visible for IPE5000).

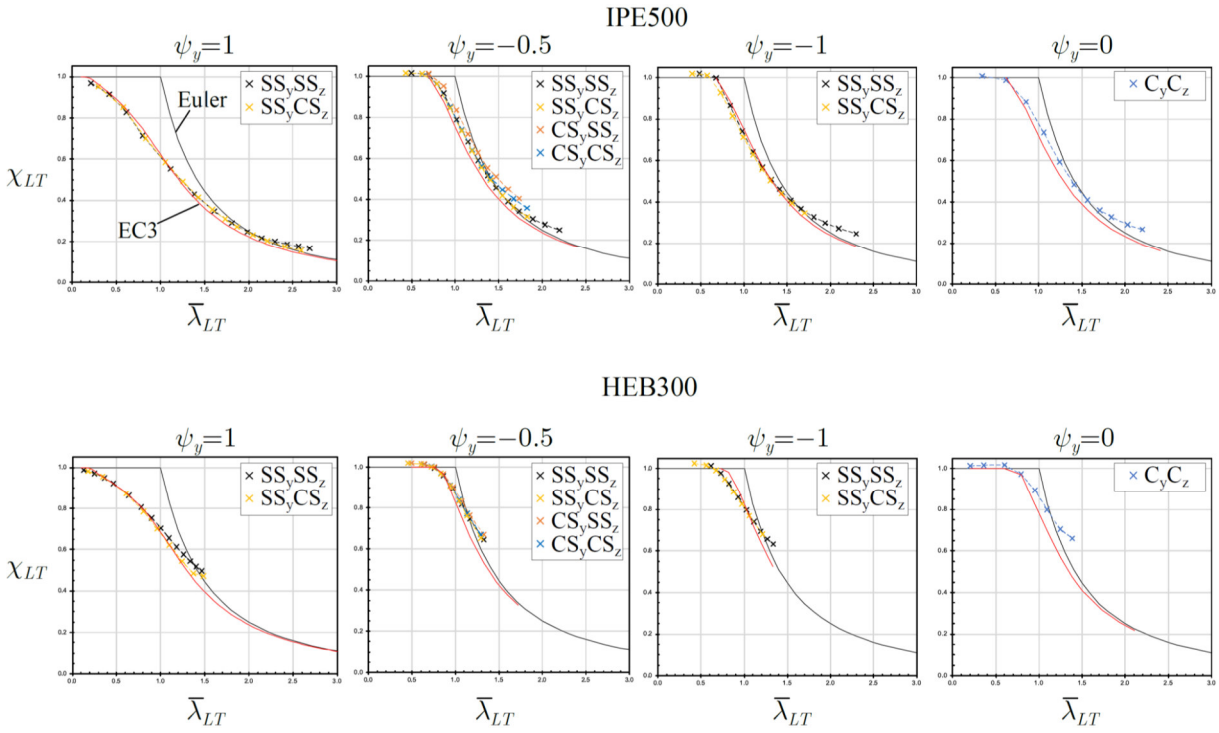

Figure 2: Buckling strength for uniaxial bending

3. GNA and GMNA under biaxial bending

3.1 Simply supported members under uniform moment

Attention is turned first to the "benchmark" case: simply supported members (SS_ySS_z) subjected to uniform moments ($\psi_y = \psi_z = 1$). For this case, Kaim (2004) derived second-order elastic stress resultants at mid-span by introducing several simplifying assumptions (e.g. the displacements follow a half sine wave shape). These resultants can be written as

$$\begin{aligned} M_y^{II} &= M_y, \\ M_z^{II} &= M_z f_z, \quad f_z = \frac{1-\beta m_{cr}^2}{1-m_{cr}^2}, \\ B^{II} &= \frac{M_z}{M_y}\frac{\pi^2 E I_w}{L^2} f_B, \quad f_B = \frac{m_{cr}^2(1-\beta)}{1-m_{cr}^2}, \end{aligned} \tag{5}$$

where M_y^{II} and M_z^{II} are the second-order moments, B^{II} is the second-order bimoment, $m_{cr} = M_y/M_{cr}$, $\beta = I_z/I_y$ (minor/major second moments of area) and I_w is the section warping constant. In this simplified solution, (i) the major axis moment M_y is unchanged, (ii) the minor axis moment M_z is amplified through function f_z and (iii) a bimoment is developed, which is inversely proportional to the square of the span, L^2. It is worth noting that the amplification function f_z is considerably different from the standard amplification function for axial force, $1/(1 - P/P_{cr})$, particularly for sections with high β values.

Fig. 3 shows a comparison between the analytical solution (5) and "exact" GNA/GMNA results, for $\bar{\lambda}_{LT} = 1,2$ and $\alpha = 11^o$, 45^o, 79^o. The stress resultants are normalized with respect to the

corresponding first yield values, i.e., $m_{el,y} = M_y^{II}/M_{el,y}$, $m_{el,z} = M_z^{II}/M_{el,z}$ and $b_{el} = B^{II}/B_{el}$. The horizontal lines in the graphs indicate the first yield loads (i.e., the condition $m_{el,y} + m_{el,z} + b_{el} = 1$) obtained with the analytical solution and GNA. These results deserve the following remarks:

(i) Overall, the analytical formulas provide reasonably accurate results, particularly for IPE500. In fact, except for HEB300 and $\bar{\lambda}_{LT} = 2$, accuracy is only lost for m_{cr} values above the yield lines. It should be also noted that the first yield lines in each graph are very close, with the single exception of the HEB300, $\bar{\lambda}_{LT} = 2$ $\alpha = 45^o$ case.

(ii) The comparison of the GNA solutions for $\bar{\lambda}_{LT} = 1$ and 2 shows that the latter cases involve lower bimoments, as predicted by Eq. (5) — recall that B^{II} is inversely proportional to L^2.

(iii) The GMNA curves attain their maxima naturally above the yield lines, but in a few cases quite close. At the maxima, a comparison of the GMNA and GNA stress resultants shows that they are quite close (sometimes virtually coincident), even if for the GMNAs, in general, $m_{el,z}$ is higher, while $m_{el,y}$ and b_{el} are lower. Therefore, not all GMNA stress resultants increase with respect to those of a GNA.

(iv) It should be noted that the bimoment cannot be generally discarded, at least for the IPE500.

3.2 Beams with $\psi_y = 1$, $\psi_z = -0.5$

Consider the $\psi_y = 1, \psi_z = -0.5$ case, which allows two different boundary conditions: SS_ySS_z and SS_yCS_z. Only IPE500 sections are investigated, since they are more affected by LT buckling (smaller β values).

As in the previous section, Fig. 4 displays the analytical solution (5) and "exact" GNA/GMNA results, for $\bar{\lambda}_{LT} = 1, 2$ and $\alpha = 11^o$, 45^o, 79^o. The normalized stress resultants displayed concern the most stressed cross-section, according to the function $m_{el,y} + m_{el,z} + b_{el}$. It should be remarked that the curves in some cases have "stepped" configuration due to a change in the most stressed cross-section in consecutive load increments. Note that, comparing the two support schemes, the analytical solution provides the same $m_{el,y}$ and $m_{el,z}$ curves but different b_{el}, since the lengths are different for the same slenderness. The following conclusions can be drawn from these results:

(i) Concerning the analytical solution, (I) it does not lead to accurate $m_{el,z}$,as it overestimates M_z^{II}, (II) as in the benchmark case, $M_y^{II} \approx M_y$ up until the maximum GMNA load and (III) the bimoment is quite accurately captured for SS_yCS_z, while it is greatly overestimated for SS_ySS_z. These differences explain why the first yield (horizontal) lines corresponding to the analytical solution are lower (sometimes considerably) than those calculated from GNAs.

(ii) Comparing the GNA results for the two supports, both M_z^{II} and B^{II} are higher for SS_yCS_z (higher as m_{cr} increases), while M_y^{II} is very similar except for $\alpha = 11^o$, in which cases it is lower for high m_{cr} and well beyond the GMNA maximum loads. This explains why the GMNA maximum loads are lower for SS_yCS_z.

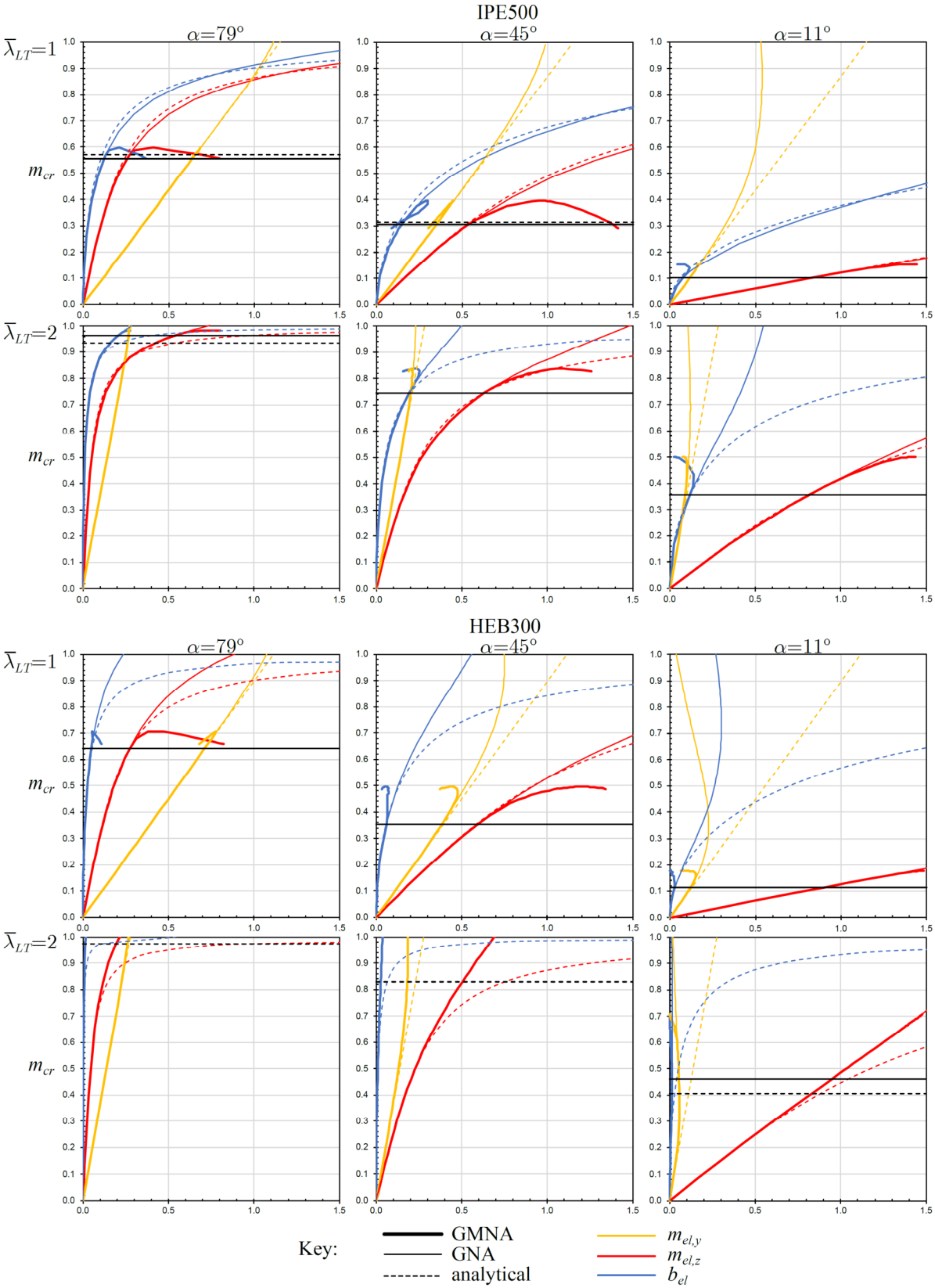

Figure 3: The benchmark case (GNA and GMNA)

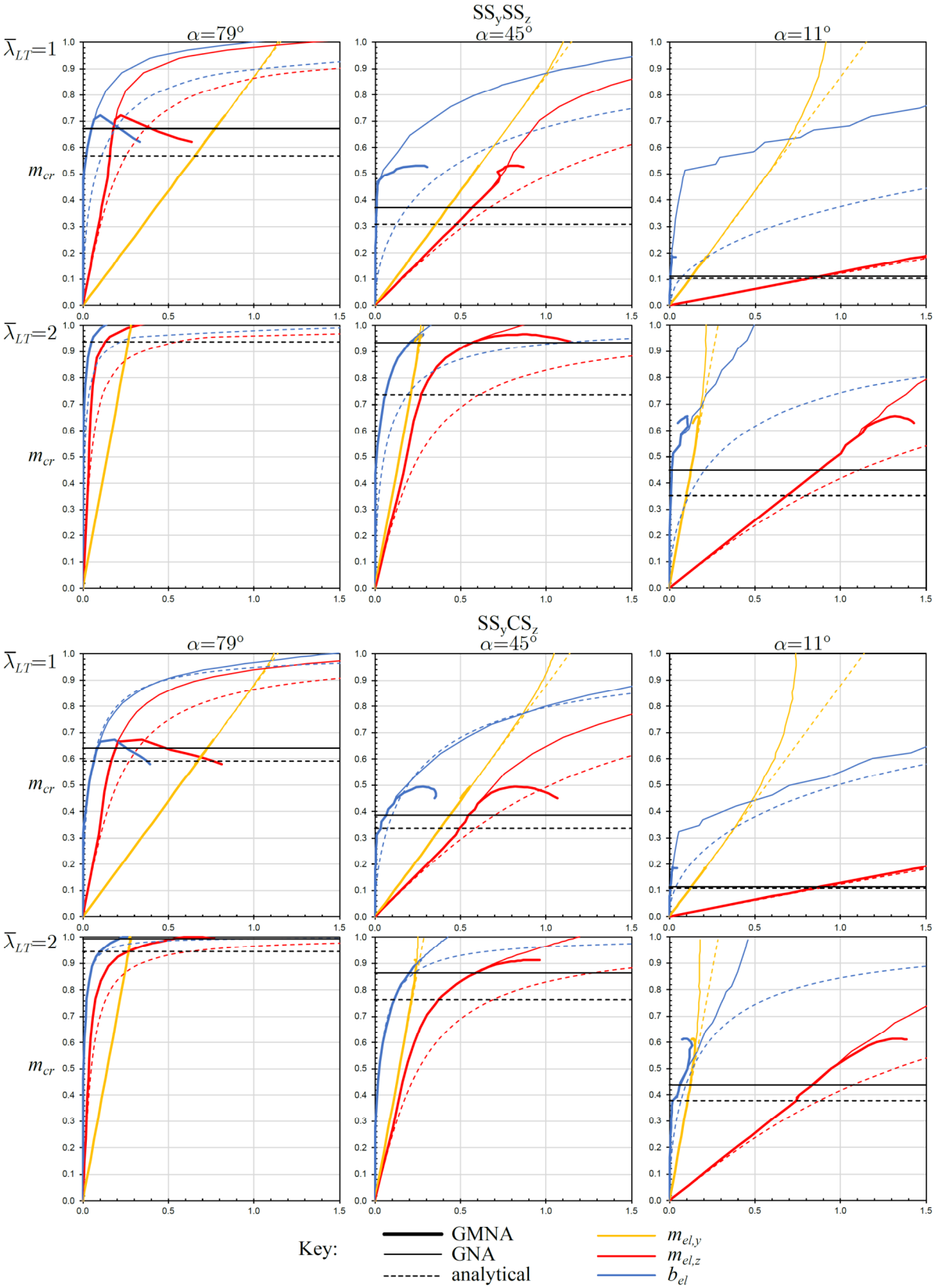

Figure 4: GNA and GMNA of IPE500 beams with $\psi_y = 1$ and $\psi_z = -0.5$

(iii) Comparing the GMNA and GNA stress resultants at the maxima shows that $m_{el,y}$ are virtually coincident, $m_{el,z}$ are very close but sometimes slightly higher for GMNA and b_{el} can be slightly higher or lower. Once more, the bimoment cannot be discarded.

Fig. 5 summarizes the maximum loads obtained so far, in m_y-m_z space, together with the cross-section plastic interaction $m_y^2 + m_z = 1$ of Eurocode 3. Naturally, the benchmark case leads to the lowest loads, but there is some difference between the two support conditions for $\psi_y = 1$, $\psi_z = -0.5$, with SS_yCS_z leading to the lowest maximum loads (between 2 and 9 % lower), due to the increased moments and bimoments, as already pointed out.

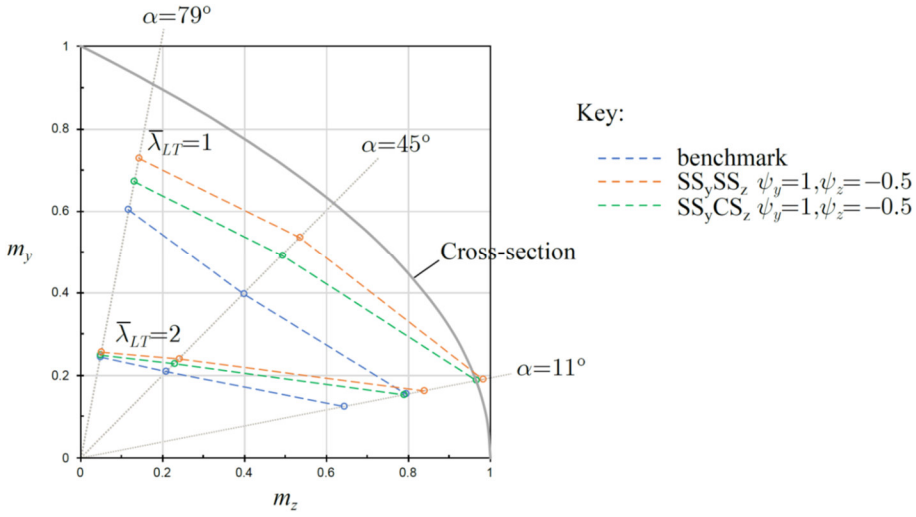

Figure 5: GMNA maximum loads

The results presented in this section show that, even though the boundary conditions are reflected in $\bar{\lambda}_{LT}$, this is not sufficient to characterize the problem, as additional effects are developed. In fact, when comparing the SS_yCS_z and SS_ySS_z cases for $\psi_y = 1$, $\psi_z = -0.5$, even though the former is statically indeterminate, it leads to lower strengths owing to higher M_z^{II} and B^{II}.

4. GMNIA under biaxial bending

The "true" buckling strength is assessed in this section, accounting for geometric imperfections and residual stresses (see Fig. 1). GMNIA results for all the cases shown in Fig. 3 (excluding $\psi_y = -1$) are presented, considering $\bar{\lambda}_{LT} = 0.5, 1.0, 1.5$ and, for IPE500, also $\bar{\lambda}_{LT} = 2.0$.

The results are grouped in Fig. 6, as a function of the cross-section type and ψ_y value. The exact cross-section interaction curve is also provided. In some cases the strength falls above M_{cr} and was capped at this value. These results prompt the following remarks:

(i) Almost all curves exhibit a pronounced convexity, even if in some cases double curvature is observed. Therefore, in these cases, a simple linear interaction formula $m_y/\chi_{LT} + m_z = 1$ can be used, as it generally falls on the safe side.

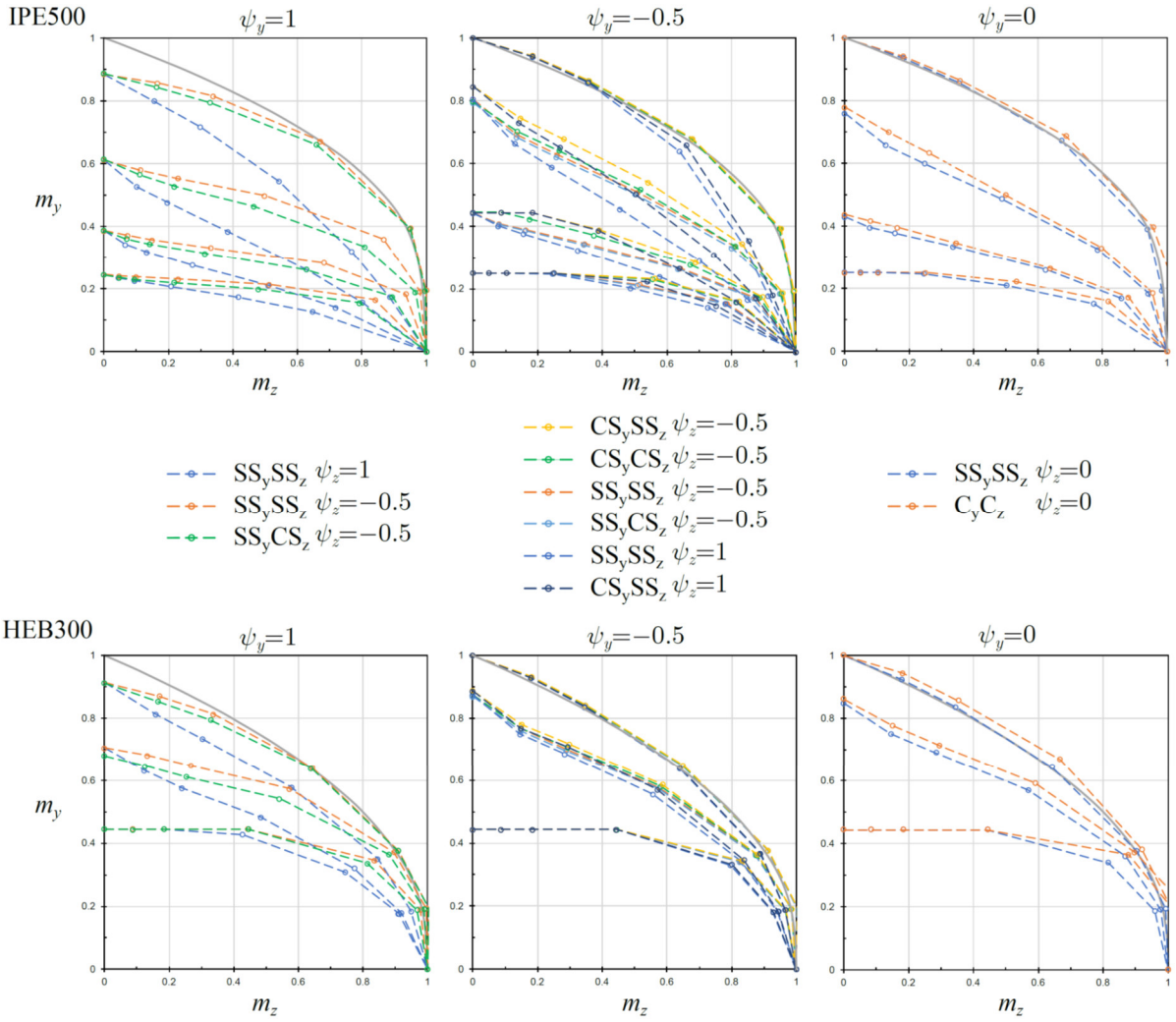

Figure 6: GMNIA maximum loads

(ii) For the same slenderness, unsurprisingly, the "benchmark" case is the most detrimental, generally followed by the $\psi_y = 1, \psi_z = -0.5$ cases, as they correspond to the lowest χ_{LT} values. The remaining cases have very similar curves, particularly for HEB300. However, it is worth noting that, for IPE500 and $\psi_y = -0.5$, some scatter is observed, with upper/lower bounds corresponding to CS$_y$SS$_z$ $\psi_z = -0.5$ and SS$_y$SS$_z$ $\psi_z = 1$, respectively.

(iii) As previously concluded, out of the two $\psi_y = 1, \psi_z = -0.5$ cases, it is the SS$_y$CS$_z$ support scheme that leads to the lowest strengths, thus using the values of the simply supported case is not on the safe side. The remaining cases with the same bending moment diagrams are discussed next, but it should be noted that the differences are more significant for the IPE500 section.

(iv) For $\psi_y = \psi_z = -0.5$, the SS$_y$SS$_z$ and SS$_y$CS$_z$ virtually match and lead to the lowest strength. However, as in the previous case, SS$_y$CS$_z$ provides lower (but in this case only slightly) values. For CS$_y$CS$_z$ a very slight strength increase is observed (most notably for IPE500 and $\bar{\lambda}_{LT} = 1.5$), while CS$_y$SS$_z$ shows the highest values, thus once more CS$_z$ leads to lower values

when compared with SS_z. It is also worth noting that the CS_y cases have a significant increased strength over the SS_y ones with the same "z" supports.

(v) For $\psi_y = -0.5$, $\psi_z = 1$, there is a significant difference between the two supports, with SS_ySS_z leading to significant lower strengths.

(vi) For $\psi_y = \psi_z = 0$, the cantilever case exhibits slightly higher values and the simply supported results can be safely adopted.

(v) The curvature of the interaction curves can be categorized as follows (smaller to higher): (I) cases with $\psi_z = 1$, (II) cases with $\psi_y = \psi_z \neq 1$ and (III) $\psi_y = 1$, $\psi_z = -0.5$.

Finally, it is worth remarking that, for $\psi_y = -0.5$, SS_ySS_z with the same slenderness and bending moment diagrams generally leads to lower strength values (for IPE500 sometimes too safe). For end-supported beams with the same bending moment diagrams, (i) for the same "y" boundary conditions, CS_z leads to lower strength values than SS_z, and (ii) for the same "z" boundary conditions, CS_y leads to higher strength values than SS_y. Finally, in each graph, the lowest values always correspond to $\psi_z = 1$ (which implies SS_z supports).

5. A note on the Eurocode 3 formulas

Presently, there are two sets of formulas for beam-columns in Eurocode 3 Part 1-1 (CEN 2005), the so-called "method 1" and "method 2" formulas. Without the partial factor for resistance, for the case of biaxial bending, they can be cast as

$$\begin{aligned} k_{yy}\frac{1}{\chi_{LT}}m_y + k_{yz}m_z \leq 1, \\ k_{zy}\frac{1}{\chi_{LT}}m_y + k_{zz}m_z \leq 1. \end{aligned} \tag{6}$$

The cross-section resistance at the member ends must also be checked, since Eqs. (6) can yield strength values above this limit. These formulas were obtained from the results of numerical studies concerning SS_ySS_z single span members. For beams with compact sections and susceptible to torsional deformations, it can be shown that one obtains

$$\begin{aligned} k_{yy} &= \left(\max\left(\frac{1}{w_y}, 1 - \frac{(w_y-1)a_{LT}\bar{\lambda}_0^2 m_y m_z}{2\chi_{LT}}\right)\right)^{-1}, \\ k_{yz} &= \frac{0.6C_{mz}\sqrt{\frac{w_z}{w_y}}}{\max\left(\sqrt{\frac{0.36}{w_y w_z}}, 1 - \frac{10(w_z-1)a_{LT}\bar{\lambda}_0^2 m_y}{(\bar{\lambda}_z^4+5)\chi_{LT}}\right)}, \\ k_{zy} &= \frac{0.6\sqrt{\frac{w_y}{w_z}}}{\max\left(\sqrt{\frac{0.36}{w_y w_z}}, 1 - \frac{2(w_y-1)a_{LT}\bar{\lambda}_0 m_y m_z}{(\bar{\lambda}_z^4+0.1)\chi_{LT}C_{mz}}\right)}, \\ k_{zy} &= C_{mz}, \end{aligned} \tag{7}$$

for method 1 and

$$
\begin{aligned}
k_{yy} &= C_{my}, \\
k_{yz} &= 0.6C_{mz}, \\
k_{zy} &= \min\left(0.6 + \bar{\lambda}_z, 1\right), \\
k_{zz} &= C_{mz},
\end{aligned}
\tag{8}
$$

for method 2, where C_m are the standard equivalent uniform moment factors pertaining to each moment diagram, $\bar{\lambda}_z$ is the non-dimensional slenderness for flexural buckling about the weak axis, $w_j = W_{pl,j}/W_{el,j} \leq 1.5$, $a_{LT} = 1 - J/I_y \geq 0$ and $\bar{\lambda}_0$ is the non-dimensional slenderness for LT buckling due to uniform bending.

Although the method 1 formulas are quite involved, it should be highlighted that only the effect of the M_z shape is considered, through C_{mz} (the effect of the M_y shape is accounted for in $\bar{\lambda}_{LT}$ and χ_{LT}). This effect is beneficial as C_{mz} decreases, as is the case of $\psi_z = -0.5$, which leads to $C_{mz} = 0.685$. In m_y-m_z space, the end points are given by

$$
\begin{aligned}
&\left(m_y = 0, m_z = \frac{1}{0.6C_{mz}}\sqrt{\frac{w_y}{w_z}}\right) \quad \text{and} \quad \left(m_y = \chi_{LT}, m_z = 0\right), \\
&\left(m_y = 0, m_z = \frac{1}{C_{mz}}\right) \quad \text{and} \quad \left(m_y = \frac{\chi_{LT}}{0.6}\sqrt{\frac{w_z}{w_y}}, m_z = 0\right),
\end{aligned}
\tag{9}
$$

and it should be noted that $C_{mz} < 1$ allows $m_z > 1$.

The method 2 interaction formulas are linear in m_y-m_z space. The second equation generally governs (if $\bar{\lambda}_z \geq 0.4$ it always governs) and its end points are given by

$$
\left(m_y = 0, m_z = \frac{1}{C_{mz}}\right) \quad \text{and} \quad \left(m_y = \chi_{LT}, \quad m_z = 0\right). \tag{10}
$$

Once again, only C_{mz} is accounted for and a change of sign of the bending moment diagram has a beneficial effect ($C_{mz} < 1$). Also note that the cross-section geometry (e.g. HEB or IPE) is not considered in this method (no w_j and a_{LT} parameters). For the cases addressed in this paper $C_{mz} = 0.6 + 0.4\psi_z \geq 0.4$ if the ends are laterally braced, otherwise $C_{mz} = 0.9$.

Fig. 7 compares the GMNIA results for $\psi_y = -0.5$ with the strength predictions of the Eurocode 3 methods 1 and 2. Only the IPE500 case is considered. For method 1, the beam lengths were taken as those of the SS_z case. The left graph shows the results for $\psi_z = -0.5$ and all slenderness values, considering the code coefficients, whereas the right graph includes $\psi_z = 1$ but focuses on $\bar{\lambda}_{LT} = 1.0$, to assess the influence of C_{mz}.

The left graph shows that both methods can yield unsafe strength predictions, particularly method 2. On the other hand, method 1 can lead to excessively safe values. The right graph shows that using $C_{mz} = 1$ ($\psi_z = 1$) generally leads to safe (in many cases excessively safe) strength values but, for method 1, some unsafe results are also obtained for SS_ySS_z $\psi_z = 1$. Note that using $C_{mz} = 1$ in method 2 leads to the linear interaction $m_y/\chi_{LT} + m_z = 1$.

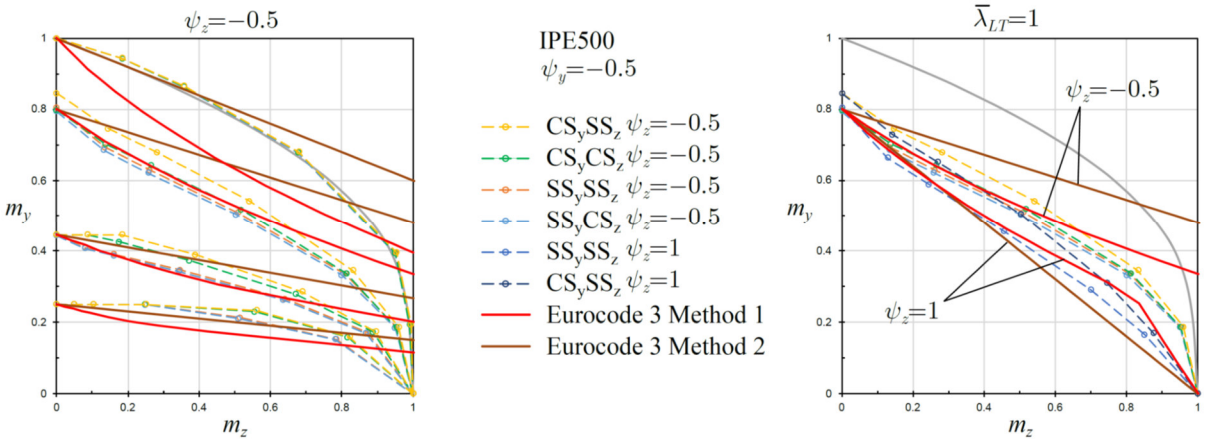

Figure 7: Comparison between GMNIA maximum loads and Eurocode 3 strength predictions

6. Concluding remarks

This paper presented the results of a numerical investigation concerning the lateral-torsional buckling behavior and strength of compact steel I-section beams subjected to biaxial bending due to end moments or forces, having various support conditions (namely other than simply supported). Although only a limited number of cases was considered, the following remarks deserve to be highlighted:

(i) The new Eurocode 3 approach for simply supported members under major axis bending provides quite accurate and generally safe strength values for beams with other support conditions, provided that $\bar{\lambda}_z$ is calculated for a simply supported member with the same $\bar{\lambda}_{LT}$ value.

(ii) GNAs and GMNAs analyses show that, for biaxial bending, significant second-order bimoments can be developed. These bimoments tend to decrease for longer beams and wide flange sections. While the major axis moment is not significantly altered, the minor axis one can also suffer an amplification. However, even for the benchmark case of simply supported beams subjected to uniform bending, this amplification is much lower than that of beam-columns.

(iii) Even though the boundary conditions are reflected in $\bar{\lambda}_{LT}$, additional effects need to be accounted for. For instance, for SS$_y$CS$_z$ and SS$_y$SS$_z$ IPE500 beams with $\psi_y = 1$, $\psi_z = -0.5$, for the same slenderness, the former leads to lower strengths owing to higher M_z^{II} and B^{II}. This case shows that the development of accurate interaction formulas should not be exclusively based on the analysis of simply supported members.

(iv) Since the strength curves for biaxial bending generally exhibit a pronounced convexity, a simple linear interaction $m_y/\chi_{LT} + m_z = 1$ can be used.

(v) The Eurocode 3 methods 1 and 2 can yield unsafe strength predictions even for the simply supported cases. Method 2 leads to more unsafe strength predictions for the cases considered. Method 1 can lead to excessively safe values. However, using $C_{mz} = 1$ ($\psi_z = 1$) generally leads to safe (in many cases excessively safe) values.

One final word to mention that work is in progress to expand the present study to other loading and support cases.

Acknowledgments

This work is part of the research activity carried out at Civil Engineering Research and Innovation for Sustainability (CERIS) and has been funded by Fundação para a Ciência e a Tecnologia (FCT) in the framework of project UIDB/04625/2020.

References

Boissonnade, N., Greiner, R., Jaspart, J., Lindner, J. (2006). *Rules for Member Stability in EN 1993-1-1. Background Documentation and Design Guidelines*, ECCS, Brussels, Belgium.

CEN (2005). *EN 1993-1-1:2005, Eurocode 3: Design of Steel Structures — Part 1-1: General Rules and Rules for Buildings*. Belgium, Brussels: CEN.

Gonçalves, R., Camotim, D. (2004). "On the application of beam-column interaction formulae to steel members with arbitrary loading and support conditions." *Journal of Constructional Steel Research*, 60(3-5), 433-450.

Gonçalves, R. (2019). "An assessment of the lateral-torsional buckling and post-buckling behaviour of steel I-section beams using a geometrically exact beam finite element." *Thin-Walled Structures*, 143, 106222.

Gonçalves, R. (2020). "On the Lateral-Torsional Elastic Post-Buckling and Strength of Channel Steel Beams." *International Journal of Structural Stability and Dynamics*, 20(12), 2050135.

Gonçalves, R., Ritto-Corrêa, M. (2022). "On the modelling of simple supports in geometrically exact thin-walled beam finite elements using a rotation vector parametrization of finite rotations." *Thin-Walled Structures*, 172, 108922.

Greiner, R., Taras, A. (2010). "New design curves for LT and TF buckling with consistent derivation and code-conform formulation." *Steel Construction*, 3(3), 176-186.

Kaim, P. (2004). *Spatial buckling behaviour of steel members under bending and compression*. PhD thesis, Technische Universitat Graz.

Ofner, R. (1997). *Traglasten von Staben aus Stahl bei Druck und Biegung*. PhD thesis, Technische Universitat Graz.

Taras, A., Greiner, R. (2010). "New design curves for lateral–torsional buckling – proposal based on a consistent derivation." *Journal of Constructional Steel Research*, 66(5), 648-663.

Ziemian, R. (2010). *Guide to Stability Design Criteria for Metal Structures*. John Wiley & Sons.